

Supplementary Information

**Directly grown high-performance WO<sub>3</sub> films by a novel one-step hydrothermal method with significantly improved stability for electrochromic applications**

Jianbo Pan, Yi Wang, Rongzhong Zheng, Maotong Wang, Zhongquan Wan, Chunyang Jia\*,

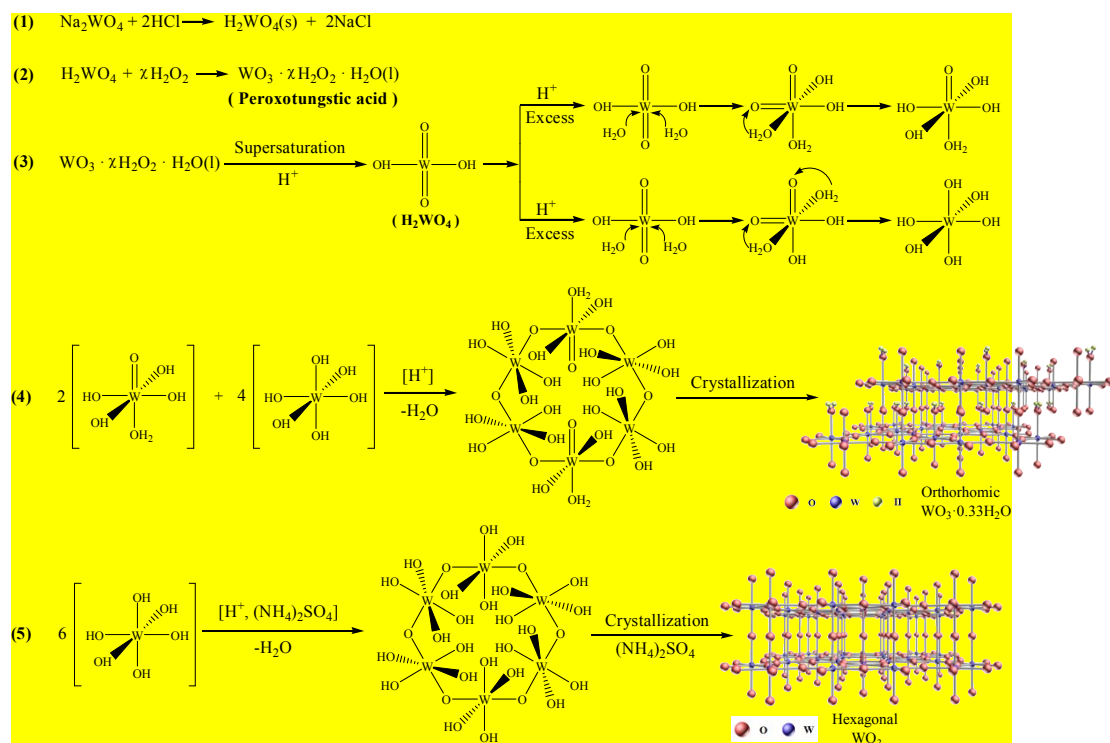
Xiaolong Weng, Jianliang Xie and Longjiang Deng

*State Key Laboratory of Electronic Thin Films and Integrated Devices, National Engineering Research Center of Electromagnetic Radiation Control Materials, School of Electronic Science and Engineering, University of Electronic Science and Technology of China, Chengdu 610054, P. R. China*

Scheme S1 shows the pertinent synthesis processes for hexagonal WO<sub>3</sub> (hex-WO<sub>3</sub>) and orthorhombic WO<sub>3</sub>·0.33H<sub>2</sub>O (ort-WO<sub>3</sub>·0.33H<sub>2</sub>O) crystals. First of all, the yellow precipitate (H<sub>2</sub>WO<sub>4</sub>) was formed by adding HCl (3 M) solution to the sodium tungstate solution. After H<sub>2</sub>WO<sub>4</sub> dissolved in hydrogen peroxide (H<sub>2</sub>O<sub>2</sub>), a stable peroxopolytungstic acid solution was obtained.<sup>1</sup> Under acid hydrothermal condition, WO<sub>2</sub>(OH)<sub>2</sub> was precipitated from the precursor solution when solution reached oversaturated state, and excess H<sup>+</sup> ions made it transform into polycondensation precursor monomers in hydration procedure, including WO(OH)<sub>4</sub>(OH<sub>2</sub>)<sup>2</sup> and W(OH)<sub>6</sub> monomers. Six monomers could be condensed to form a six-membered ring structure, then further nucleated. Finally, after the crystal nucleus reached a critical size, the crystals of ort-WO<sub>3</sub>·0.33H<sub>2</sub>O and hex-WO<sub>3</sub> were obtained respectively by further crystalized growth.

---

\* Corresponding author. Tel.: +86 28 83201991; Fax: +86 28 83202569. Email: [cyjia@uestc.edu.cn](mailto:cyjia@uestc.edu.cn) (C. Y. Jia)



Scheme S1. Proposed synthetic route for the formation of orthorhombic  $\text{WO}_3 \cdot 0.33\text{H}_2\text{O}$  and hexagonal  $\text{WO}_3$ .

The chemical composition of FTO-coated glass surface was characterized by FT-IR spectra, as shown in Fig. S1. An obvious broad peak at  $3370 \text{ cm}^{-1}$  is ascribed to O-H. The bands at regions between  $2800\text{-}3650 \text{ cm}^{-1}$  and  $1700\text{-}1400 \text{ cm}^{-1}$  are assigned to O-H stretching and O-H bending, respectively,<sup>3, 4</sup> which confirm that the surface of FTO-coated glass is active and rich in hydroxyl (-OH) groups. Particularly, the peaks of  $2920 \text{ cm}^{-1}$  and  $2347 \text{ cm}^{-1}$  can be attributed to some residual organic matter.

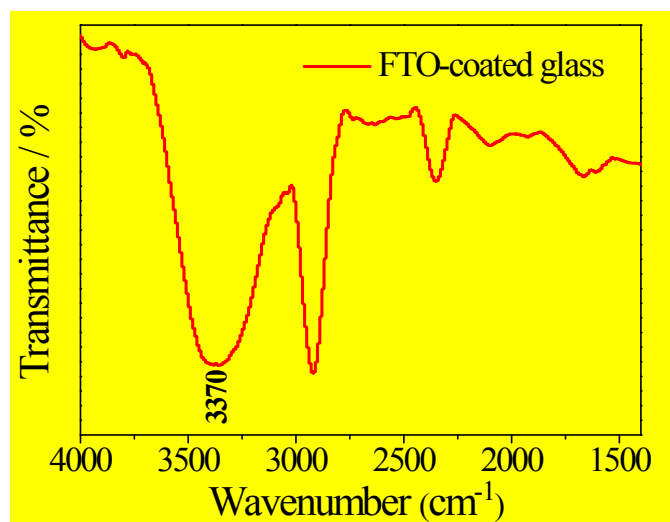
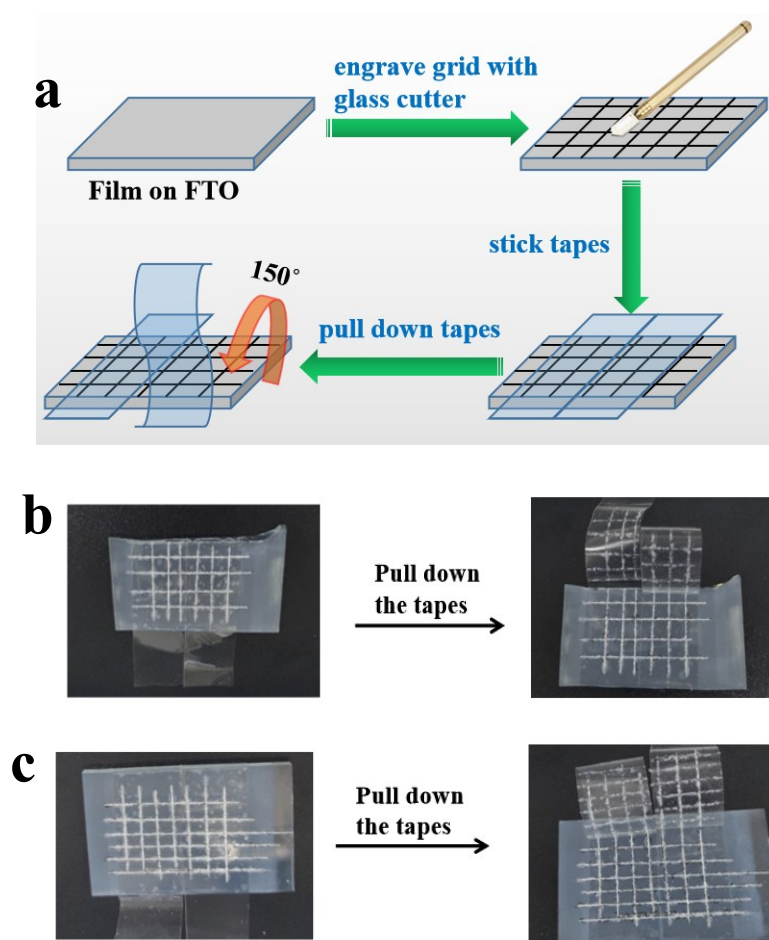


Fig. S1 The FT-IR spectra of FTO-coated glass.

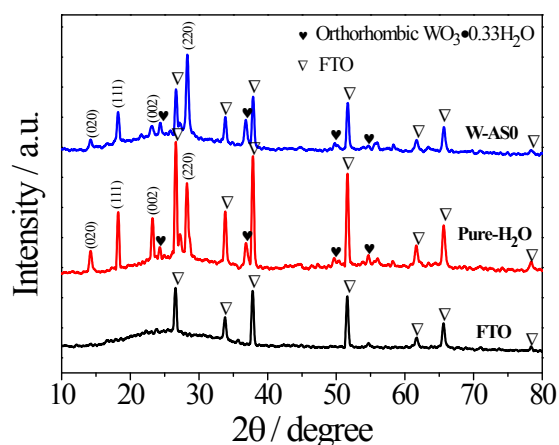
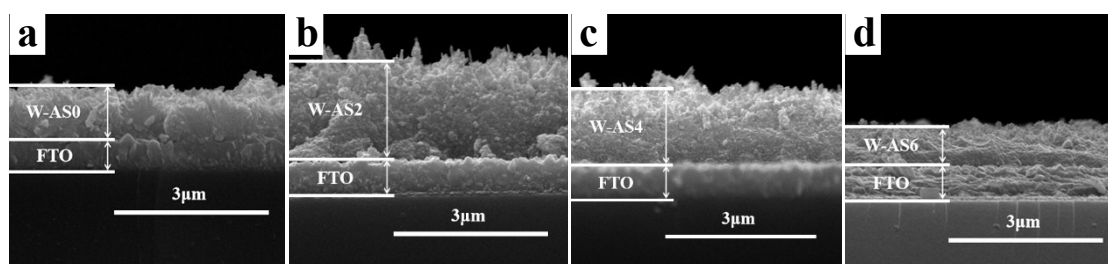
The adhesive force of  $\text{WO}_3$  films with (W-AS0) and without (pure- $\text{H}_2\text{O}$ ) glycerol were tested via a simple grid-sticking method. As shown in Fig. S2a, first of all, using glass cutter to engrave grids (2mm \* 2mm) on films. Secondly, sticking the tapes (3M #600) firmly and covering at least one small grid. After 2-5 minutes, pulling down the tapes at 150 degree, and evaluating the damage level of each film according to Table S1. The damage of W-AS0 film occurred only at the intersection of cutting lines, but pure- $\text{H}_2\text{O}$  film at the edges and intersection of cutting lines **simultaneously**. Therefore, the damage of W-AS0 film and pure- $\text{H}_2\text{O}$  film could be judged as 4B and 3B, respectively. It **could** be confirmed that glycerol can strengthen the adhesive force between  $\text{WO}_3$  film and FTO.



**Fig. S2** (a) Schematic illustration of grid-sticking method; The contrast test of adhesive force of films: (b) with glycerol (W-AS0 film), (c) without glycerol (pure- $\text{H}_2\text{O}$  film).

**Table S1** The damage grade check list of film

Damage grade	Damage description
5B	The edge of the cutting line is smooth and the mesh does not fall off at all.
4B	Fine powder drops off at the intersection of cutting lines, and the affected area is less than 5%.
3B	Fine powder drops off at the edge and intersection of the cutting lines, and the affected area ranges from 5% to 15%.
2B	Flakes fall off at the edge and grid of cutting lines, and the affected area ranges from 15% to 35%.
1B	Strip flakes falling off and the whole grid falling off at the edge of the cutting line, and the affected area ranges from 35% to 65%.
0B	More serious film shedding that 1B

**Fig. S3** XRD patterns for FTO-coated glass, pure-H<sub>2</sub>O and W-AS0 films.**Fig. S4** Cross-sectional SEM images of WO<sub>3</sub> films: (a) W-AS0, (b) W-AS2, (c) W-AS4, (d) W-AS6.**Table S2** The thickness of each film

Sample	W-AS0	W-AS2	W-AS4	W-AS6
Thickness (μm)	1.11	1.88	1.58	0.81

The pore size distribution of each structure as shown in Fig. S5, it can be found that there are peaks at 3~5 nm in both W-AS0 and W-AS4 structures, but not in W-

AS2 structure, which indicates the W-AS2 structure does not contain 3~5 nm pore.

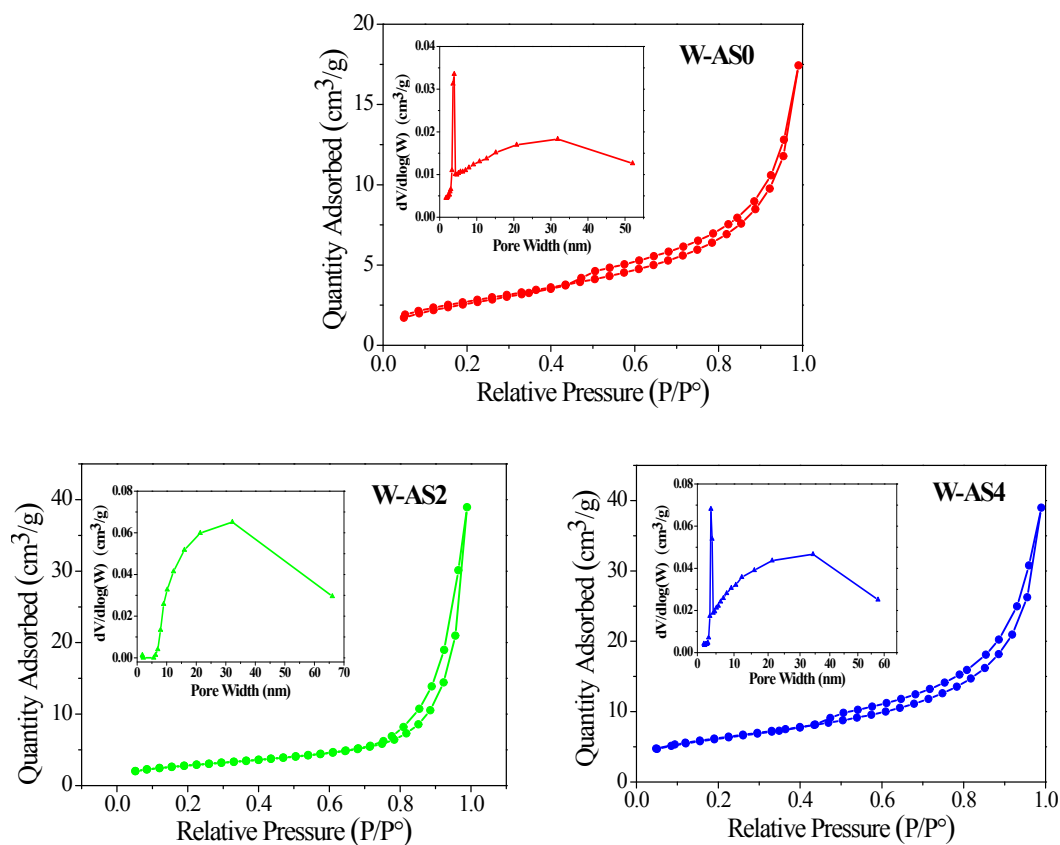
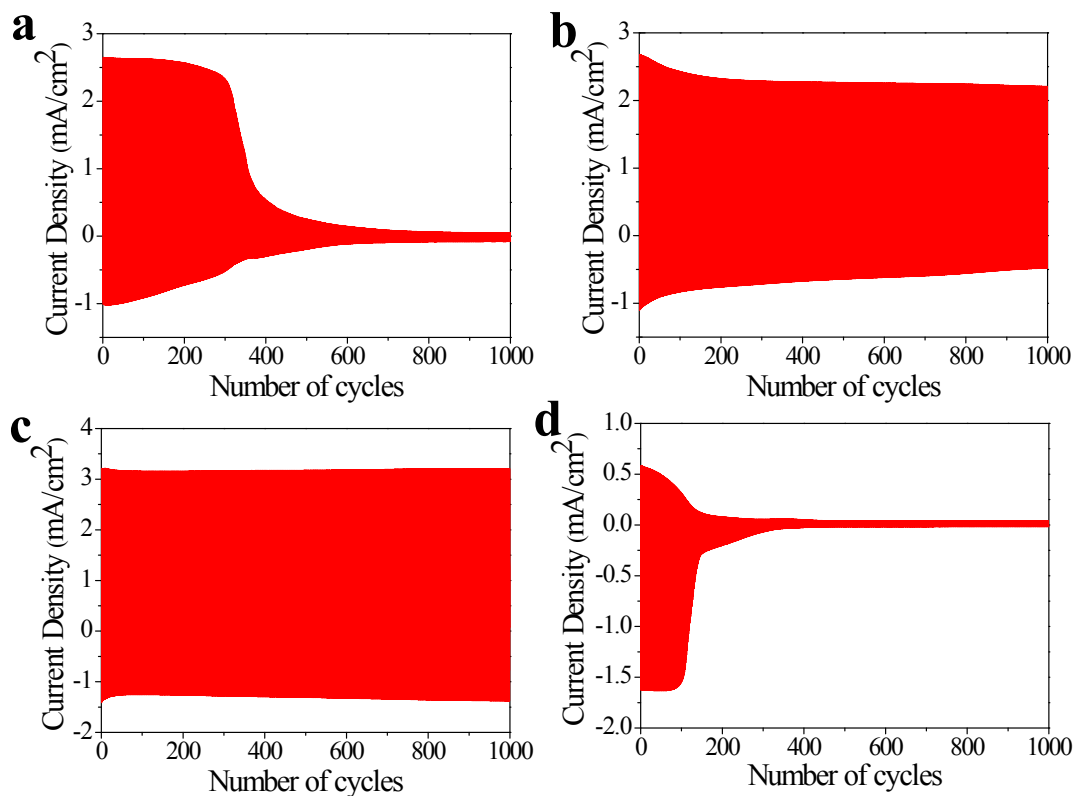


Fig. S5 N<sub>2</sub> (77 K) adsorption/desorption isotherms linear plots (inset: pore size distribution).

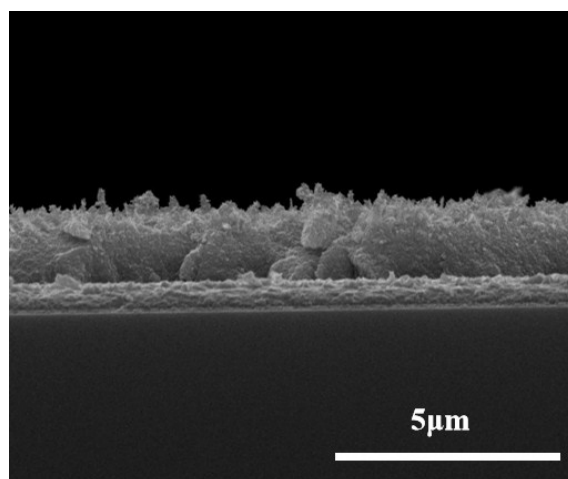
Table S3 The specific surface area of different structures

Sample	W-AS0	W-AS2	W-AS4	W-AS6
Specific Surface Area (m <sup>2</sup> /g)	10.1	10.3	22.5	

Note: Due to the low yields of W-AS6 powder with low crystallinity, the surface area could not be tested.

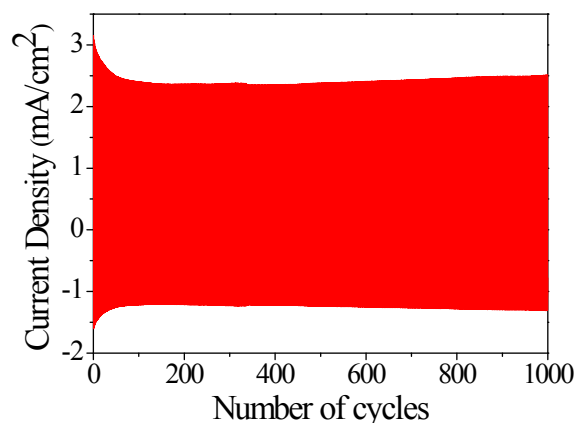


**Fig. S6** The step chronoamperometric cyclic curves of WO<sub>3</sub> films with different amounts of (NH<sub>4</sub>)<sub>2</sub>SO<sub>4</sub> at -1.5 V (colored, 10 s) and +2.0 V (bleached, 10 s): (a) W-AS0, (b) W-AS2, (c) W-AS4, (d) W-AS6.



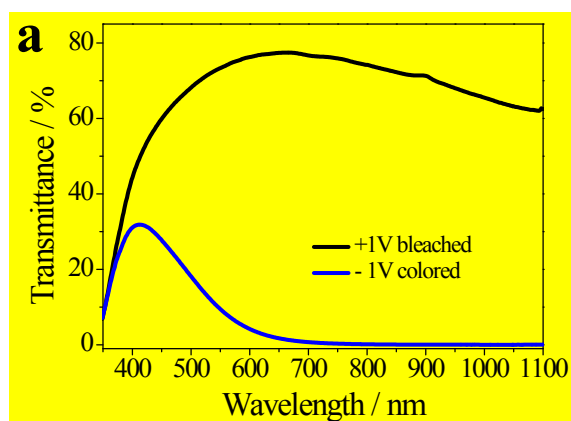
**Fig. S7** Cross-sectional SEM image of W-AS4<sub>seed</sub> film.

Fig. S8 shows the cyclic stability of W-AS4<sub>seed</sub> film in 1000 cycles. As same as W-AS4 film, the W-AS4<sub>seed</sub> film is in activation stage within at least 1000 cycles.



**Fig. S8** The step chronoamperometric cyclic curve of W-AS4\_seed film at -1.5 V (colored, 10 s) and +2.0 V (bleached, 10 s).

Fig. S9 shows the electrochromic performance of W-AS4\_seed film. At 630 nm wavelength, the transmittance modulation range of W-AS4\_seed film under  $\pm 1.0$  V voltages was about 75.1%, which was lower than W-AS4 film (78.1%). The bleaching time ( $t_b$ ) and coloration time ( $t_c$ ) were calculated to be 8 s and 5 s, respectively, which were slower than the ones of W-AS4 film (6/5 s for bleaching/coloration). The coloration efficiency was calculated to be  $45.1 \text{ cm}^2 \text{ C}^{-1}$ , while it was  $56.5 \text{ cm}^2 \text{ C}^{-1}$  in W-AS4 film. Thus, we could conclude that the self-seeded hydrothermal method is better than crystal-seed-assisted hydrothermal method.



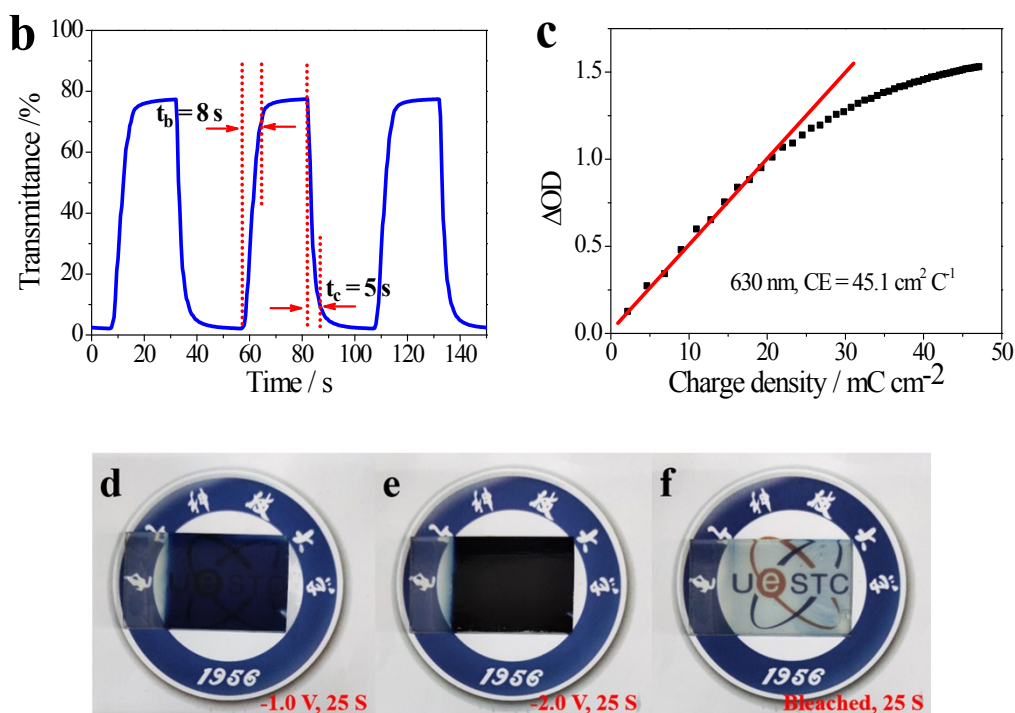


**Fig. S9** The electrochromic performance of W-AS4\_seed film: (a) UV-vis transmittance spectrum of colored and bleached states between 350 nm and 1100 nm, (b) Switching time and transmittance variation curves between colored and bleached states at 630 nm,  $\pm 1.0$  V bias, (c) Variation of the optical density ( $\Delta OD$ ) versus charger density ( $Q$ ); Digital photographs of the W-AS4\_seed film at different stages: (d) colored at  $-1.0$  V for 25 s, (e) colored at  $-2.0$  V for 25 s, (f) bleached at  $2.0$  V for 25 s.

**Table S4** The electrochromic performances comparison of W-AS4 film with and without crystal seed layer

Name	$\Delta T$ [%/nm]	Tc/Tb [s]	CE [cm <sup>2</sup> C <sup>-1</sup> ]
W-AS4 film	78.1	5.0/6.0	56.5
W-AS4_seed film	75.1	5.0/8.0	45.1

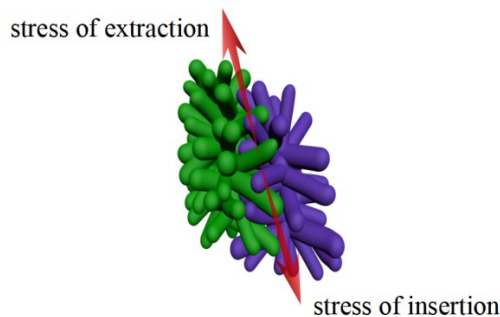


**Fig. S10** Schematic illustration of the possible interlocking force in coral-like nanostructure of W-AS4 film.

Fig. S11 shows the electrochemical and electrochromic properties of PB film. All

the above tests were carried out in 1 M LiClO<sub>4</sub>/PC electrolyte by conventional three-electrode test method. In CV curve of PB film, there are two obvious peaks at -0.2 V and +0.6 V, which correspond to the reduction and oxidation reactions, respectively.<sup>5</sup> The electrochromic properties of PB film were tested at ±0.6 V. The switching time and transmittance variation curve between colored and bleached states at 630 nm shows  $t_c/t_b$  was 2.5/6 s.

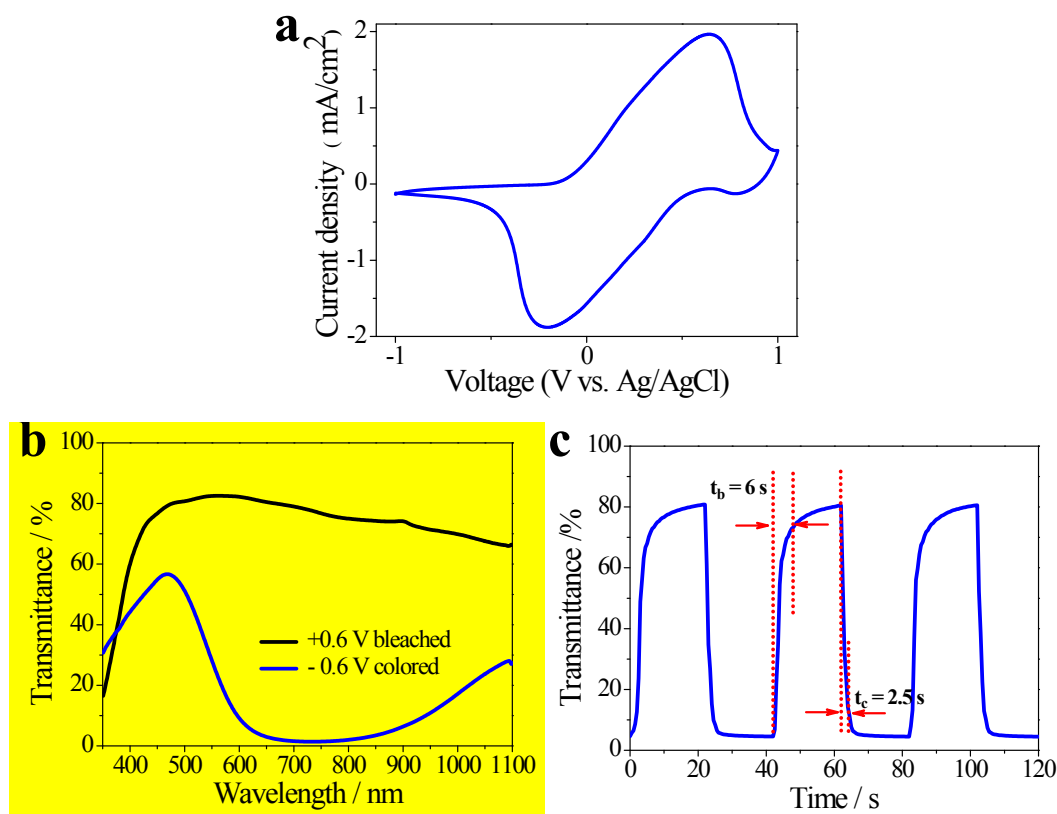


**Fig. S11** (a) CV curve of PB film; (b) UV-vis transmittance spectrum of PB film in colored and bleached states between 350 nm and 1100 nm; (c) Switching time and transmittance variation curves between colored and bleached states at 630 nm, ±0.6 V bias.

## References

- 1 Z. Jiao, X. W. Sun, J. Wang, L. Ke and H. V. Demir, *J. Phys. D: Appl. Phys.*, 2010, 43, 285501.
- 2 D. Mandal, P. Routh and A. K. Nandi, *Small*, 2018, 14, 1702881.
- 3 L. Zhu, W. L. Ong, X. Lu, K. Zeng, H. J. Fan and G. W. Ho, *Small*, 2017, 13, 1700084.
- 4 A. Phuruangrat, D. J. Ham, S. J. Hong, S. Thongtem and J. S. Lee, *J. Mater. Chem.*, 2010, 20, 1683-1690.
- 5 Z. Jiao, J. Wang, L. Ke, X. Liu, H. V. Demir, M. F. Yang and X. W. Sun, *Electrochim. Acta*, 2012, 63, 153-160.